

Differential charge detection for quantum-dot cellular automata

Islamshah Amlani,^{a)} Alexei O. Orlov, Gregory L. Snider, and Gary H. Bernstein
Department of Electrical Engineering, University of Notre Dame, Notre Dame, Indiana 46556

(Received 28 May 1997; accepted 21 July 1997)

We report direct measurements of the charging diagram of a nanoscale series double-dot system at low temperatures. Our device consists of four metal dots, with two of them in series forming a double-dot, and the other two serving as electrometers for the double-dot system. This configuration allows us to externally detect all possible charge transitions within a double-dot system. Specifically, we can detect charge redistribution in the double-dot, which corresponds to shift of an electron between two dots, using differential signal from the two electrometers. We discuss possible applications as an output stage for quantum-dot cellular automata architecture. © 1997 American Vacuum Society. [S0734-211X(97)04806-3]

I. INTRODUCTION

Coupled mesoscopic structures utilizing the Coulomb blockade (CB) phenomenon have been studied in various metal and semiconductor systems.¹⁻⁶ Various investigators have pointed out that coupled dots in the CB regime can perform useful computing functions.⁷⁻¹² One such computational paradigm, known as quantum-dot cellular automata (QCA), was proposed by Lent *et al.*⁸⁻¹⁰ A basic QCA cell can be built of two series-connected dots separated by tunneling barriers and capacitively coupled to an identical double-dot. If the cell is biased such that there are two excess electrons within the four dots, these electrons will be forced to opposite corners by Coulomb repulsion. The two possible electron configurations, i.e., the polarization states of the system, can represent logic “0” and “1.” Properly arranged, arrays of these basic cells can implement Boolean logic functions.

Critical to any device or system whose operation depends upon the motion of single electrons is a means of detecting the positions of individual electrons. It has been shown that a single electron transistor (SET) can be used to detect charge variation in a nearby dot.^{13,14} In previous experiments, the Coulomb interaction of electrons within a double-dot has been inferred exclusively from their series conductance.⁴⁻⁶ A detection scheme that can probe the polarization state of the double-dot externally, and with high sensitivity, has not heretofore been developed.

We present direct measurement of the internal charge state of a double-dot system, a precursor to the basic QCA cell. Specifically, our charge detection technique is sensitive not only to the charge variation of individual dots but also to the more subtle exchange of one electron between the two dots. This important property of our detection scheme makes it suitable for sensing the polarization state of a QCA cell. In this article, we describe the basic principle of our detection strategy. Issues regarding the detection accuracy which depend on the coupling parameters of a QCA cell are discussed in Ref. 15.

II. EXPERIMENT

Figure 1(a) shows a schematic diagram of our metal dot system. It consists of two islands in series, D_1 and D_2 , connected by a tunnel junction, with each island capacitively coupled to an electrometer-dot, E_1 and E_2 , respectively. An interdigitated design is used for the coupling capacitors, C_{11} and C_{22} , in order to make the electrometers sensitive to small charge variations on the double-dot.

Sample preparation consisted of two levels of optical lithography and a third level of electron beam lithography on an oxidized Si surface. The first level of optical lithography defined a thin interconnect (150 Å of Pt) between the second optical level, consisting of a 3000-Å-thick layer of Au (to assist in bonding) that formed the bonding pads, and the *e*-beam level (Al). Fabrication of Al/AIO_x/Al tunnel junctions was carried out in the third level which involved electron beam lithography and double angle shadow evaporation of Al.¹⁶ Figure 1(b) shows a field emission scanning electron microscope (FESEM) micrograph of the device. The bottom electrode metal, 25 nm thick, was oxidized *in situ*, followed by 50 nm of Al to form the top electrode. The two islands labeled D_1 and D_2 between the three (60×60 nm²) tunnel junctions are 1.4 μm long. In the vicinity of each dot are “driver gate” electrodes labeled *A* and *B*. Each island of the double dot system is also capacitively coupled to a SET (labeled E_1 and E_2) with an island length of 1.1 μm.

Measurements were carried out in a dilution refrigerator (25 mK) using standard ac lock-in techniques. A 4 μV ac excitation voltage at a frequency of 20 Hz was used to measure the conductance of the double-dot and the electrometers. A magnetic field of 1 T was applied to suppress the superconductivity of Al. The typical tunnel resistance of a junction, based on current–voltage (*I*–*V*) measurements of the electrometers at 4.2 K, is approximately 200 kΩ. The total capacitance of the electrometer-dots, C_{Σ} , extracted from the charging energy ($E_C \sim 80 \mu\text{eV}$), is approximately 1 fF.

Initial experiments were performed to extract the lithographic and parasitic capacitance parameters of the various parts of the circuit. Capacitances between various gates and islands, determined from the periods of the Coulomb blockade oscillations (CBOs),¹ are listed in Table I. The double

^{a)}Electronic mail: Islamshah.Amlani.1@nd.edu

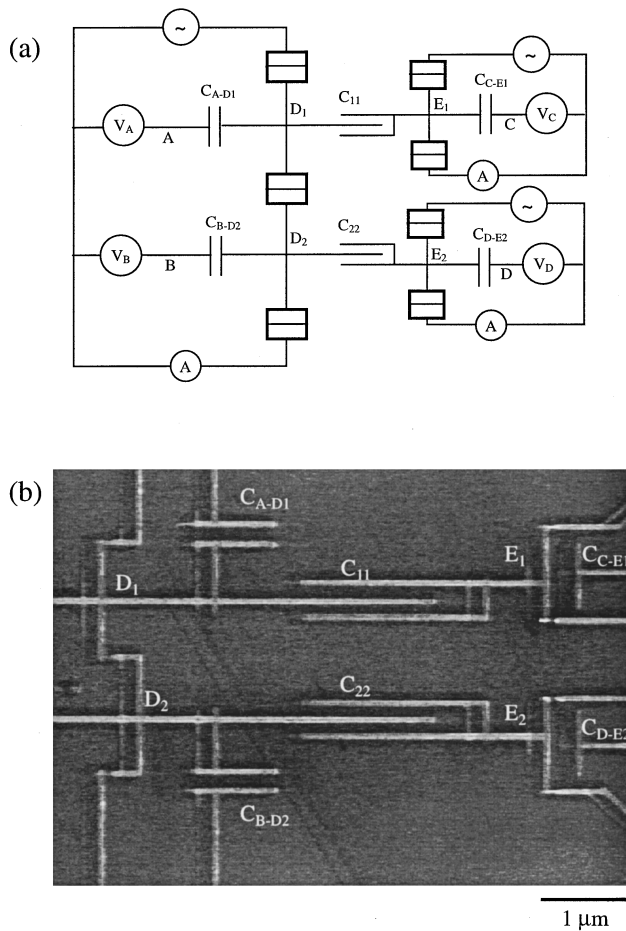


FIG. 1. (a) Schematic diagram of the device structure. Capacitance parameters of different parts of the device are listed in Table I. The capacitances of the coupling capacitors C_{11} and C_{22} are approximately 10% of the total capacitances of the electrometers, C_{Σ} . The circuit used to compensate for parasitic capacitance between the driver gates A/B and the electrometer islands E_1/E_2 is not shown. (b) FESEM micrograph of the device.

dot structure was used as a gate electrode to measure the capacitance of the coupling capacitors, C_{11} and C_{22} .

In subsequent experiments, the charge on the double-dot structure was varied by sweeping driver gates A and B . Conductances through the double-dot and both SET electrometers were measured simultaneously as a function of driver gate voltages. To ensure an identical response from the electrometers, their operating points were set to be equal to each other on a rising edge of their current versus island charge characteristics. The sensitivities of the electrometers, as expected from Ref. 13, were proportional to C_{11} and C_{22} . As mentioned above, these coupling capacitors were designed to be relatively large in order to increase the sensitivity of the electrometers (Table I), yet constitute a sufficiently small fraction of C_{Σ} for the electrometers to act as noninvasive probes.¹⁴

Our external circuitry was more involved than that shown in Fig. 1(b) in order to compensate for parasitic capacitance. It can be seen from Table I that the parasitic capacitances between the driver gates and the electrometer islands are non-negligible. This undesirable parasitic capacitance can be

TABLE I. Lithographic and parasitic capacitances between various gates and islands shown in Fig. 1(a), measured from the period of the Coulomb blockade oscillations.

Type	Capacitor	Approx. cap. (aF)
Lithographic	C_{A-D1}	47.7
Lithographic	C_{B-D2}	49.5
Lithographic	C_{C-E1}	29
Lithographic	C_{D-E2}	26.6
Lithographic	C_{11}	106
Lithographic	C_{22}	106
Parasitic	C_{A-E1}	21
Parasitic	C_{A-E2}	8
Parasitic	C_{B-E1}	9.69
Parasitic	C_{B-E2}	21.3
Parasitic	C_{C-E2}	7.5
Parasitic	C_{D-E1}	7.5

diminished significantly by using a multilayer fabrication process described in Ref. 17. In our experiment, we applied inverted compensation voltages proportional to V_A and V_B to gates C and D in order to suppress the influence of the parasitic capacitances. Using this charge compensation technique, we were able to observe up to 100 periods in the electrometer conductances due to discrete variations of the coupled island charges, without inducing extra charge on them due to the driver gates.¹⁴ We believe that this charge compensation technique will not be necessary in a real QCA circuit since very small biases are needed on the driver gates to perform computation and their influence on the charge state of the electrometer islands will be negligibly small.¹⁵

III. RESULTS AND DISCUSSION

Figure 2 shows a contour plot of the conductance through the double-dot as a function of driver gate voltages, V_A and V_B . The resulting charging diagram of such a measurement forms a ‘‘honeycomb’’ structure.⁵ The honeycomb boundaries (solid lines) represent the regions where a change in electron population (n_1, n_2) occurs on one or both of the dots, with n_1 and n_2 representing excess populations of D_1 and D_2 , respectively. Each hexagonal cell marks a region in which a given charge configuration is stable due to Coulomb blockade. In the interior of the cell there is no charge transport through the double dot; conductance through the double dot peaks only at the ‘‘triple points,’’ where the Coulomb blockade is lifted for both dots.

The charge configuration of the double-dot can be varied by sweeping driver gate voltages along any of the three directions shown in Fig. 2. This does not result in a significant current flow through the double-dot if the path chosen avoids triple points. For instance, along directions I and II, charge is added to only one of the dots in units of single electrons, while the population of the other dot stays constant. Charge redistribution in the double-dot takes place along direction III when the change in driver gate voltages is in opposite direction. Along this direction, electrons are shifted from one dot to the other and total charge on the double dot remains unchanged.

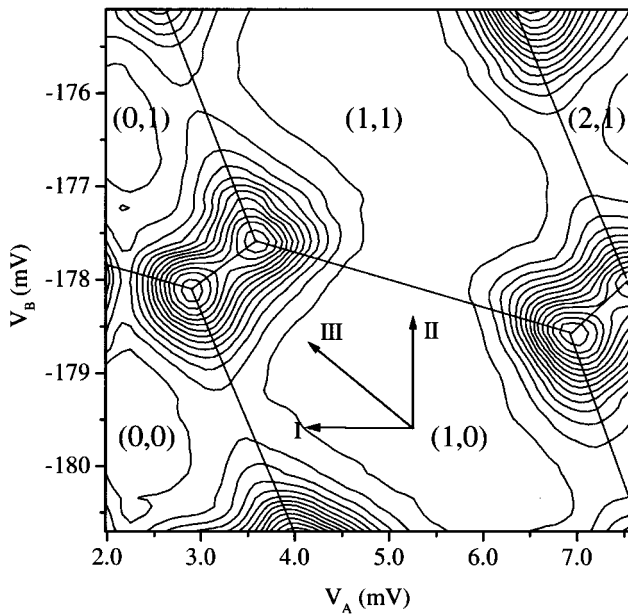


FIG. 2. Charging diagram of the double dot as a function of driver gate voltages. Charge configurations (n_1, n_2) , which represent the number of extra electrons on D_1 and D_2 , respectively, are arbitrarily chosen. Lines labeled I, II, and III show a few directions in which charge can shift between different configurations of the double dot.

Figure 3 shows gray-scale contour plots of the conductance through SET electrometers E_1 [Fig. 3(a)] and E_2 [Fig. 3(b)] as a function of the driver gate voltages, where lighter areas represent higher conductance. Superimposed on each plot are the solid lines that define the honeycomb structure of Fig. 2. The change in the conductance of each electrometer reflects the variation of the electrostatic potential in the dot capacitively coupled to it. A sharp change in the conductance of E_1 from light to dark in the horizontal direction [Fig. 3(a)] represents addition of an electron to D_1 . Similarly, sharp variation in conductance of E_2 in the vertical direction [Fig. 3(b)] indicates discrete variation of charge on D_2 . Hence, the sharpest variations in the conductances of each electrometer represent the charging of their capacitively coupled dots.

Detection of polarization change in a QCA cell is equivalent to sensing the charge redistribution in the double dot which takes place along direction III (Fig. 2). In Fig. 3, it can be seen that the transitions along this direction are detected less strongly in the electrometer signals. This is caused by the cross capacitance between D_1 (D_2) and E_2 (E_1) which makes each electrometer sensitive to both dots. Thus, charging of each dot of the series double-dot leads to oscillations in both electrometers. According to our measurements, the amplitude of oscillations in E_1 [Fig. 3(a)] due to the charging of remote dot D_2 (along the vertical direction) is approximately 30% of that due to the charging of nearby dot D_1 (along the horizontal direction). During charge redistribution in the double dot (line III in Fig. 2), the population of each dot separately changes by one electron with one dot losing an electron and the other gaining one. Consequently, the signals from the two dots are out of phase by 180° . Since the

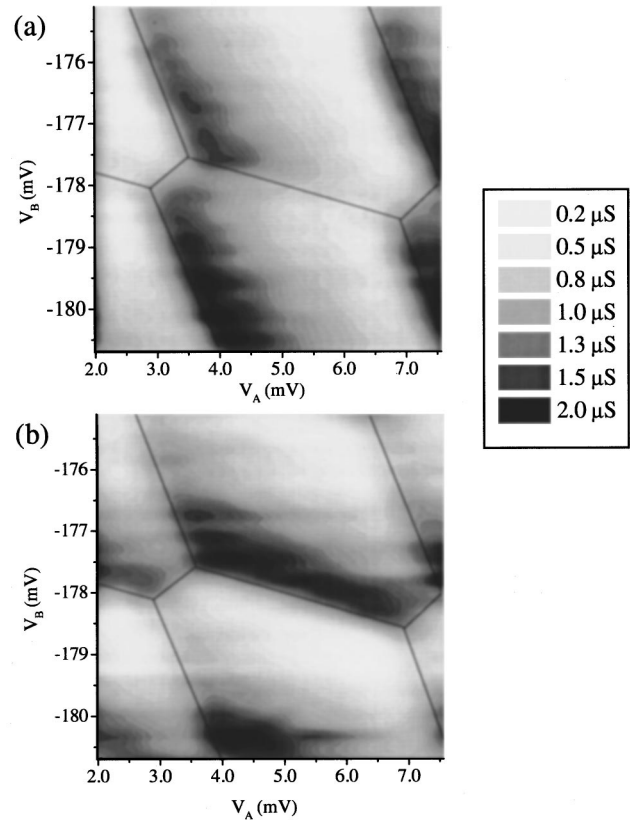


FIG. 3. Conductance of the electrometers as a function of the same driver gate voltages shown in Fig. 2 with the honeycomb boundaries of Fig. 2 superimposed. (a) Conductance of E_1 . Sharp transitions in the horizontal direction indicate a change in the population of D_1 . (b) Conductance of E_2 . Sharp transitions in the vertical direction reflect a change in the population of D_2 .

conductance of each electrometer along this direction shows superposition of the two signals, the detected signal is about 30% weaker than that along the direction I (II) in the conductance of E_1 (E_2).

Figure 4 shows honeycomb borders (solid lines) overlaid on a gray-scale contour plot of a differential signal $(G_1 - G_2)$, where G_1 and G_2 are the conductances of E_1 and E_2 , respectively. Along directions I and II in Fig. 2, the variations in the conductances of E_1 and E_2 exhibit the same phase with one stronger than the other, resulting in a suppressed differential signal. The most conspicuous transition, represented by a higher density of contour lines, occurs at the boundary between the (0,1) and (1,0) states, indicating movement of an electron from one dot to the other. As mentioned above, this is due to the phase difference (180°) in the signals of the individual electrometers along this direction, yielding a differential signal which is approximately twice as strong as the one detected by a single electrometer.

IV. SUMMARY

We have presented measurements of a series double dot and its capacitively coupled SET electrometers. Our device architecture allows us to directly observe the internal state of

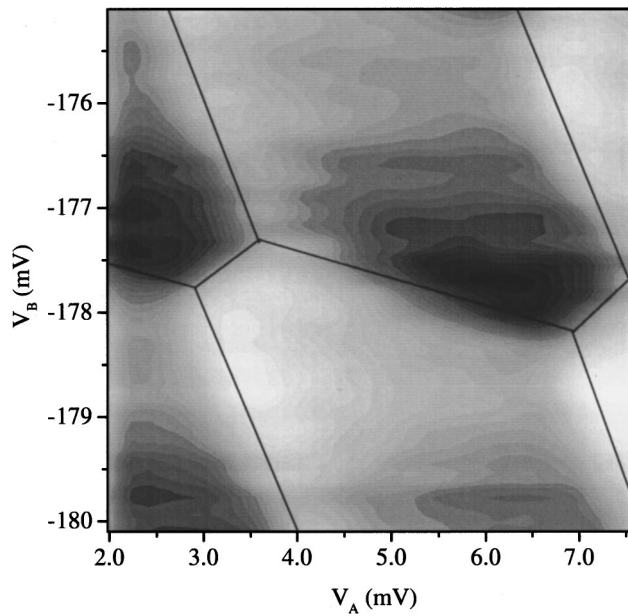


FIG. 4. Differential signal obtained from the charging diagrams of the individual electrometers. The most salient transition is in the direction of charge redistribution indicated by a higher density of contour lines.

a coupled dot system by detecting all possible charge transitions of a single electron. A differential detector that utilizes the signals from both electrometers is most sensitive to the charge redistribution in the double dot. As proposed by Lent *et al.*¹⁰ a complete implementation of QCA requires the detection of single electron motion between dots. With this investigation, we demonstrate that our differential detector can be used as an output stage of QCA.

ACKNOWLEDGMENTS

The authors are grateful to C. S. Lent and W. Porod for helpful discussions. This research was supported in part by Defense Advanced Research Project Agency and the National Science Foundation.

- ¹D. V. Averin and K. K. Likharev, in *Mesoscopic Phenomena in Solids*, edited by B. L. Altshuler, P. A. Lee, and R. A. Webb (North Holland, Amsterdam, 1991).
- ²H. van Houten, C. W. J. Beenaker, and A. A. M. Staring, in *Single Charge Tunneling*, edited by H. Grabert, and M. H. Devoret (Plenum, New York, 1992), and references therein.
- ³W. P. Kirk and M. A. Reed, *Nanostructures and Mesoscopic Systems* (Academic, Boston, 1992).
- ⁴F. R. Waugh, M. J. Berry, D. J. Mar, and R. M. Westervelt, *Phys. Rev. Lett.* **75**, 705 (1995).
- ⁵H. Pothier, P. Lafarge, C. Urbina, D. Esteve, and M. H. Devoret, *Europhys. Lett.* **17**, 249 (1992).
- ⁶T. Sakamoto, S. Hwang, F. Nihey, Y. Nakamura, and K. Nakamura, *Jpn. J. Appl. Phys., Part 1* **33**, 4876 (1994).
- ⁷J. R. Tucker, *J. Appl. Phys.* **72**, 4399 (1992).
- ⁸C. S. Lent, P. D. Tougaw, and W. Porod, *Appl. Phys. Lett.* **62**, 714 (1993).
- ⁹C. S. Lent, P. D. Tougaw, W. Porod, and G. H. Bernstein, *Nanotechnology* **4**, 49 (1993).
- ¹⁰C. S. Lent and P. D. Tougaw, *J. Appl. Phys.* **75**, 4077 (1994).
- ¹¹J. M. Martinis, M. Nahum, and H. D. Jensen, *Phys. Rev. Lett.* **72**, 904 (1994).
- ¹²P. D. Dresselhaus, L. Ji, S. Han, J. E. Lukens, and K. K. Likharev, *Phys. Rev. Lett.* **72**, 3226 (1994).
- ¹³P. Lafarge, H. Pothier, E. R. Williams, D. Esteve, C. Urbina, and M. H. Devoret, *Z. Phys. B* **85**, 327 (1991).
- ¹⁴G. Bazan, A. O. Orlov, G. L. Snider, and G. H. Bernstein, *J. Vac. Sci. Technol. B* **14**, 40 (1996).
- ¹⁵A. O. Orlov, I. Amlani, G. L. Snider, C. S. Lent, and G. H. Bernstein (unpublished).
- ¹⁶T. A. Fulton and G. H. Dolan, *Phys. Rev. Lett.* **58**, 109 (1987).
- ¹⁷E. H. Visscher, S. M. Verbrugh, J. Lindeman, P. Hadley, and J. E. Mooji, *Appl. Phys. Lett.* **66**, 305 (1994).